

Design and Analysis of Plasmonic Nanostub Filter Using Metal-Insulator- Metal (MIM) Waveguide

Suraya Mubeen

Associate Professor, CMRTC, Hyderabad, Telangana.

mail id: suraya418@gmail.com

Abstract. Metal-insulator-metal (MIM) silicon based nanostub structures have been designed and analyzed using the finite difference time-domain (FDTD) technique. An analytic model is discussed which is based on the resonance theory. Numerical results show double and single narrow band transmissions for small and long lengths of nanostub, respectively. The transmission band of the structure is controlled by varying the width and the length of the nanostub. These MIM nanostub structure can have potential applications in nanoscale high density photonic integrated circuits (PICs)

Keywords- Metal-insulator-metal (MIM), Nanostub Structure, Photonic integrated circuits (PICs), Plasmonic filter, Transmittance

1 Introduction

Recently, plasmonic structures have attracted special interest due to their ability to propagate long-range surface plasmon polaritons (LRSPPs) at optical frequencies. Surface plasmon polaritons (SPPs) are waves that originate from interaction between metallic surface electrons and electromagnetic waves [1] [2]. Several nanoscale plasmonic waveguide structures have been reported for wavelength filters, which include metallic nanowires [3,4], metallic nanoparticle arrays [5] [6], metal-insulator-metal (MIM) waveguide [7] [8]. These plasmonic structures exhibit strong field localization, easy fabrication and feasibility of integration with different optical circuits. In addition, a variety of plasmonic MIM based optical components, such as, U-shaped waveguides [9], splitters [10], switches [11] [12], Y-shaped combiners [13], couplers [14], Mach-Zehnder interferometers [15], Bragg reflecting filters [16] [17], side-coupled cavity [18], and teeth structures [8] [19] have been reported.

In this paper, an SPP based MIM silicon based nanostub structure is designed. This waveguide structure employs two semi infinite materials, a dielectric and a conductor, for implementing MIM based waveguide. The filtering characteristics of device are changed using a high dielectric constant insulating core. The structure is analyzed using finite difference time domain (FDTD) method with perfectly matching layer (PML) absorbing boundaries.

Comment [WU1]: The paper needs lot of revision. All the results plots have to be provided tidily once again.

Comment [WU2]: Role not required. Give Dept details

Comment [WU3]: Not required

Comment [WU4]: Include the paper organization following this statement

2 Characteristics of MIM Waveguide Structure

Figure 1 shows the schematic drawing of proposed MIM structure. It consists of an inner with dielectric core connected to the interface between the dielectric SiO₂ with outer metallic covering of silver (Ag). The dispersion relation of the fundamental transverse magnetic (TM) mode in a MIM waveguide is given by [12] [13] as:

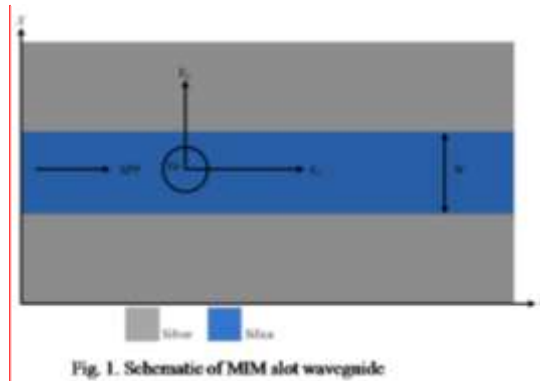
$$\varepsilon_i k_{z2} + \varepsilon_m k_{z1} \coth\left(-\frac{jk_{z1}}{2} w\right) = 0 \quad (1)$$

Where w is width of dielectric core, k_{z1} and k_{z2} are the momentum conservations

$$k_i = \varepsilon_i k_0^2 - \beta^2, \quad k_{z2} = \varepsilon_m k_0^2 - \beta^2 \quad (2)$$

Where the parameter ε_i ($= 3.9$) for SiO₂ and the frequency-dependent complex relative permittivity of Ag is characterized through the Drude model [20]:

$$\varepsilon_m(\omega) = \varepsilon_\infty - \frac{\omega_p^2}{\omega(\omega + i\gamma)} \quad (3)$$



Comment [WU5]: Do not start like this

Comment [WU6]: Screenshots are not allowed

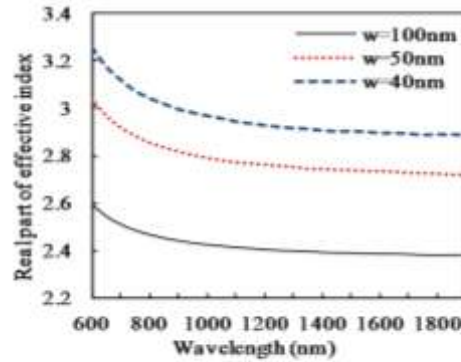


Fig. 2. Real part of the effective refractive index of a metal-insulator-metal (MIM) waveguide structure versus operating wavelength for different widths.

Where ω_p ($= 1.38 \times 10^{16}$ Hz) is the silver's bulk plasma frequency, ω is the angular frequency of the incident electromagnetic wave, and ϵ_∞ ($= 3.7$) is the dielectric constant at infinite angular frequency. Further, k_0 is the free-space wave vector and β is the propagation constant. The effective refractive index of the MIM nano-plasmonic waveguide structure is given as $n_{\text{eff}} = \beta/k_0$. Fig. 2 shows the real part of n_{eff} versus the wavelength (λ) for different SiO_2 widths (W) in MIM waveguide. The result highlights that the effective index decreases with the increase in wavelength for same w_1 , while it increases for smaller w_1 .

2.1 Plasmonic MIM Waveguide based Nanostub Filter

Schematic drawing of a single nanostub based nanoplasmonic filter is shown in Fig. 3, with $w = 250$ nm (check this dielectric width W or nanostub width w), which ensure that only fundamental TM mode is supported in optical frequency range. P and Q are the power monitors placed at 100 nm from the nanostub. Port1 acts as the input while port2 acts as the output of the filter.

The mesh sizes along x- and y- directions are set to be 5nm \times 5nm. The transmittance is defined as ratio of the transmitted (P_{out}) to incident (P_{in}) powers, i.e., $T = P_{\text{in}}/P_{\text{out}}$. The transmittance characteristic of the nanostub structure is obtained through FDTD simulation using perfect matched layers (PMLs) as absorbing boundaries. In FDTD simulations, the TM mode is launched from the input side of the waveguide as shown in Fig. 3.

Comment [WU7]: Do not add screenshots.

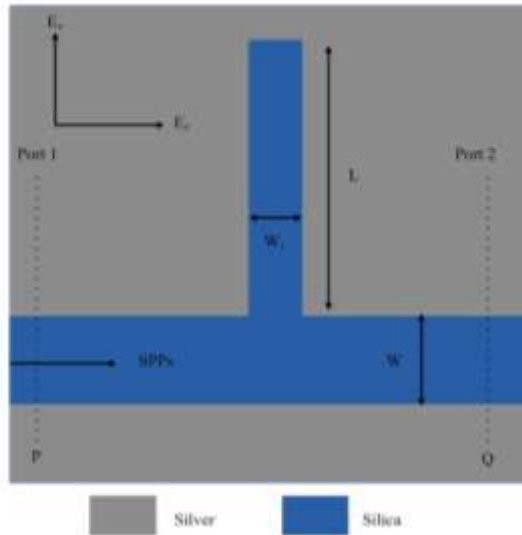


Fig. 3. Geometry of plasmonic MIM waveguide based single nanostub filter

Comment [WU8]: Same as above.

2.2 Results and Discussion

Figure 4 shows the transmission spectra of the nanostub structure with fixed stub length of $L=425\text{nm}$, width of the waveguide $W=250\text{nm}$ and nanostub's width of $w_1=15\text{nm}$. It is observed that the proposed waveguide exhibits dual stop band characteristics. The wavelength of the first dip is at 1070nm and second dip is at $\sim 1470\text{nm}$ for SiO_2 dielectric material. Here we observed that the transmittance is lower at higher wavelength for a given fixed length of the nanostub and width of the waveguide.

Comment [WU9]: Do not start like this

Figure 5 shows the transmission spectra of the nanostub structure with different nanostub lengths for a given nanostub width of $w_1=15\text{nm}$ and waveguide width of $w=250\text{nm}$. We observed that with increase in the stub length, the transmittance minima decreases and band stop wavelength shifts towards higher values.

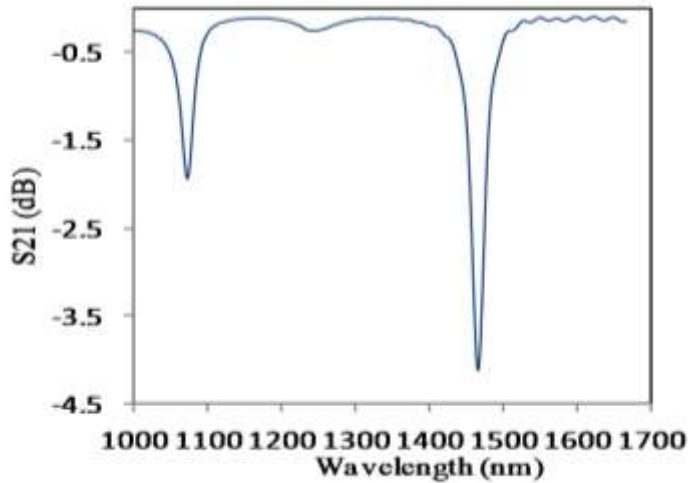


Fig. 4. Transmission coefficient of the nanostub filter structure with a wavelength.

Fig. 6, shows the transmission spectra of the nanostub structure for different waveguide widths (w) at a fixed nanostub length of $L=425$ nm and stub width $w_1=15$ nm. It shows that on increasing width of the waveguide, transmittance dip shifts towards lower values almost at same band-stop wavelength. Width of the waveguide (w) influences the transmittance characteristics of a SPP wave in the structure. Dependence of the transmittance on the separation, between upper and lower Silver plates is shown in Fig.6. The full width half maximum (FWHM) of the nanostub waveguide with widths $w=50$ and 250 nm are 39 nm and 21 nm respectively. Further, it is observed from Fig. 6, that the FWHM of the dip decreases with increase in the nanostub/gap width w . This is because of high impedance mismatch in wide gap. It also results in high reflectance at the junction between the waveguide and the nanostub [16]. Moreover, the transmittance decreases with decrease in separation w due to huge loss within narrower waveguides. Therefore, the effect of gap w is also sensitive for resonant characteristics of an SPP wave.

Comment [WU10]: Figure needs modifications

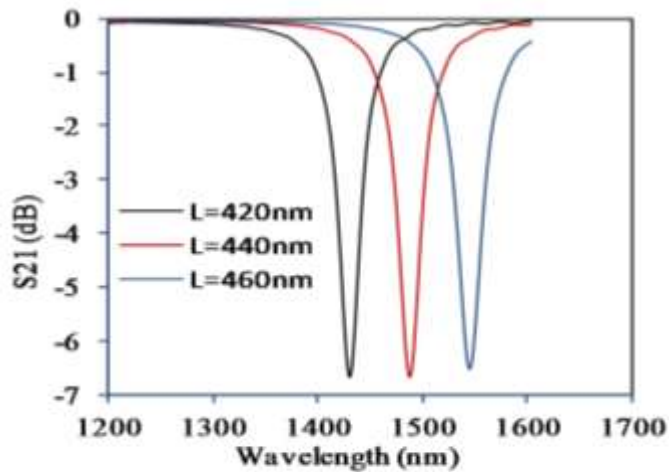


Fig. 5. Variation of transmission coefficient with wavelength as a function of stub length L .

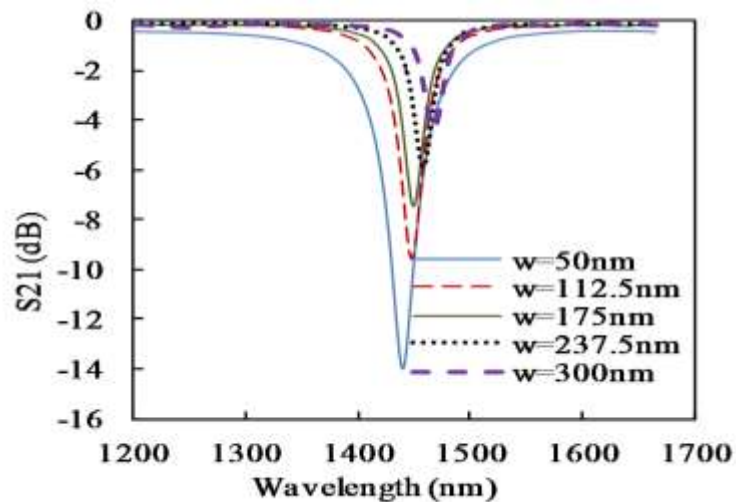


Fig. 6. Variation of transmission coefficient with wavelength as a function of width w

Generally, it is difficult to get sharp corners in a nanostub structure. Still, nanostub structures with corners at the crossings can be created using focused ion beam (FIB) technology. Hence, effect of smooth corners at crossings on transmission characteristics is of prime importance for feasible implementation of nanostub structures. In this regard, Fig. 7 shows simulated transmission characteristics versus wavelength for both the smooth and the sharp corners in

nanostub structure with fixed stub length $L = 425$ nm, stub width $w_1 = 15$ nm, and waveguide width $w = 250$ nm. From Fig. 7, it can be inferred that minima in the transmission characteristics decreases for smooth corners stub in comparison to a sharp corners stub structure.

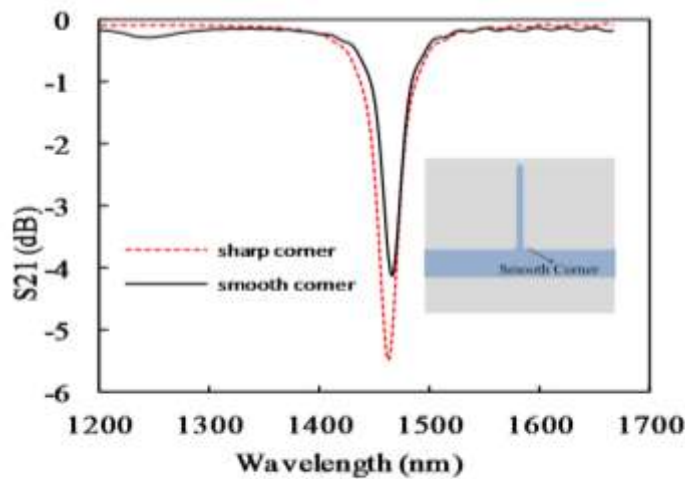


Fig. 7. Transmission coefficient of the nanostub waveguide filters with smooth and sharp corners at a fixed stub length of $L = 425$ nm, waveguide width $w = 250$ nm, stub width of $w_1 = 15$ nm

3 Conclusion

In this paper, transmittance characteristics of the surface plasmon nanostub structure are analyzed. It exhibits the functionality of a narrowband wavelength-filter. The wavelength corresponding to the transmittance dip increases with increase in the nanostub length, L . While it displays a inverse relation with the waveguide width, w or W check. Hence one can obtain filtering characteristics through the presented single nanostub based plasmonic MIM structure. Further, this filtering operation can be achieved at any operating wavelength by changing the waveguide width, w , and the nanostub length, L . Such nanostub structure opens a way to construct nanoscale high-density photonic integrated circuits (PICs).

Acknowledgement: The author acknowledge support by the Koneru Lakshmaiah Education Foundation ,Guntur, Andhrapradesh, India.

Comment [WU11]: How can you just using only the S11 and VSWR. The radiation pattern plots are required

References

1. H. Raether, *Surface Plasmon on Smooth and Rough Surfaces and Gratings*. Berlin, Germany: Springer-Verlag, 1998.
2. W. L. Barnes, A. Dereux, and T. Ebbesen, "Surface plasmon Subwavelength optics," *Nature*, vol. 424, pp. 824–830, 2003
3. J. C. Weeber, A. Dereux, C. Griad, J. R. Krenn, and J. P. Goudonnet, "Plasmon polaritons of metallic nanowires for controlling submicron propagation of light," *Phys. Rev. B*, vol. 60, pp. 9061–9068, 1999.
4. R. M. Dickson and L. A. Lyon, "Unidirectional plasmon propagation in metallic nanowires," *J. Phys. Chem. B*, vol. 104, pp. 6095–6098, 2000.
5. M. Quinten, A. Leitner, J. R. Krenn, and F. R. Aussenegg, "Electromagnetic energy transport via linear chains of silver nanoparticles," *Opt. Lett.*, vol. 23, pp. 1331–1333, 1998.
6. S.A.Maier, P. G. Kik, H. A. Atwater, S.Meltzer, E. Harel, B. E. Koel, and A. A. G. Requicha, "Local detection of electromagnetic energy transport below the diffraction limit in metal nanoparticle plasmon waveguides," *Nat. Mater.*, vol. 2, pp. 229–232, 2003.
7. Y. Matsuzaki, T. Okamoto, M. Haraguchi, M. Fukui, and A. Nakagaki, "Characteristics of gap plasmon waveguide with stub structures," *Opt. Express*, vol. 16, pp. 16314–16325, 2009.
8. Xian-Shi Lin and Xu-Guang Huang, "Tooth-shaped plasmonic waveguide filters with nanometric sizes," *Opt. Lett.*, vol. 33, pp. 2874–2876, 2008.
9. T. Lee and S.Gray, "Subwavelength light bending by metal slit structures," *Opt. Express*, vol. 13, pp. 9652–9659, 2005.
10. G.Veronis and S. Fan, "Bends and splitters in metal dielectric–metal subwavelength plasmonic waveguides," *Appl. Phys. Lett.*, vol. 87, pp. 131105-1–131105-3, 2005.
11. C. J. Min and G. Veronis, "Absorption switches in metal-dielectric-metal plasmonic waveguides," *Opt. Express*, vol. 17, pp. 10757–10766, 2009.
12. Z. Yu, G. Veronis, S. Fan, and M. L. Brongersma, "Gain-induced switching in metal-dielectric-metal plasmonic waveguides," *Appl. Phys. Lett.*, vol. 92, p. 041117, 2008.
13. H. Gao, H. Shi, C. Wang, C. Du, X. Luo, Q. Deng, Y. Lv, X. Lin, and H. Yao, "Surface plasmon polariton propagation and combination in Yshaped metallic channels," *Opt. Express*, vol. 13, pp. 10795–10800, 2005.
14. [14] H. Zhao, X.Huang, and J.Huang, "Novel optical directional coupler based on surface plasmon polaritons," *Physica. E*, vol. 40, pp. 3025–3029, 2008.
15. [15] Z. Han, L. Liu, and E. Forsberg, "Ultra-compact directional couplers and Mach-Zehnder interferometers employing surface plasmon polaritons," *Opt. Commun.*, vol. 259, pp. 690–695, 2006.
16. B.Wang and G.Wang, "Plasmon Bragg reflectors and nanocavities on flat metallic surface," *Appl. Phys. Lett.*, vol. 87, p. 013107, 2005.
17. Q. Zhang, X.-G. Huang, X.-S. Lin, J. Tao, and X.-P. Jin, "A Subwavelength coupler-type MIM optical filter," *Opt. Express*, vol. 17, pp. 7549–7554, 2009.
18. W. Lin and G. Wang, "Metal hetero waveguide superlattices for a plasmonic analog to electronic bloch oscillations," *Appl. Phys. Lett.*, vol. 91, p. 143121, 2007.
19. X.-S. Lin and X.-G. Huang, "Numerical modeling of a teeth-shaped nanoplasmonic waveguide filter," *J. Opt. Soc. Am. B*, vol. 26, pp. 1263–1268, 2009.
20. [20] J. Tao, X.-G. Huang, and S.-H. Liu, "Optical Characteristics of Surface Plasmon Nanonotch Structure," *J. Opt. Soc. Am., B*, Vol. 27, No. 7, July, 2010.
21. P. B. Johnson and R. W. Christy, "Optical constants of the noble metals," *Phys. Rev.*, vol. 6, pp. 4370–4379, 1972